Static potential in baryon

D.S. Kuzmenko

Institute of Theoretical and Experimental Physics, 117218, B. Cheremushkinskaya 25, Moscow, Russia

Abstract

The baryon static potential is calculated in the framework of field correlator method and is shown to match the recent lattice results. The effects of the nonzero value of the gluon correlation length are emphasized.

1. The static potential is a key quantity in the calculations of spectra and wave functions of baryons in the potential models [1], as well as in the QCD string approach [2]. On the other hand the static potential is generated by the gluon forces of QCD and therefore sheds the light on the profound properties of strong interactions. Accurate numerical calculations of static potential in baryon performed in lattice QCD last years [3], [4] induced new significant growth of interest to the structure of the gluon forces in baryon.

The results of calculations of the baryon potential in the framework of the method of the field correlators (MFC) [5] are presented in this report. We set the correspondence of this potential to lattice one and underline fundamental effects of strong interactions — the confinement of color charges and definite value of the correlation length of the gluon fields, which reveal themselves in the behavior of baryon potential.

2. The static potential is expressed through the Wilson loop \mathcal{W}_B according to the relation

$$V_B = -\lim_{T \to \infty} \frac{1}{T} \ln \mathcal{W}_B, \tag{1}$$

and that is why we are proceeding now to the calculations of Wilson loop. The baryon Wilson loop is shown in Fig. 1 and is defined as follows,

$$\mathcal{W}_B = \left\langle \frac{1}{6} \epsilon_{\alpha\beta\gamma} \epsilon^{\alpha'\beta'\gamma'} \Phi^{\alpha}_{\alpha'}(C_1) \Phi^{\beta}_{\beta'}(C_2) \Phi^{\gamma}_{\gamma'}(C_3) \right\rangle, \tag{2}$$

where the parallel transporter or Schwinger line Φ is given as

$$\Phi_{\beta}^{\alpha}(x, y, C) = (P \exp ig \int_{C} A_{\mu} dz_{\mu})_{\beta}^{\alpha}. \tag{3}$$

The average of the Wilson loop over the vacuum fields using the nonabelian Stokes theorem and bilocal (two-point) approximation is performed in [5], and the result reads as

$$W_B = \exp\left\{-\sum_{i=1}^3 \frac{1}{2} \int_{S_i} \int_{S_i} d\sigma_{\mu_1 \nu_1}(x) d\sigma_{\mu_2 \nu_2}(x') \mathcal{D}_{\mu_1 \nu_1, \mu_2 \nu_2}(x - x') + \right\}$$

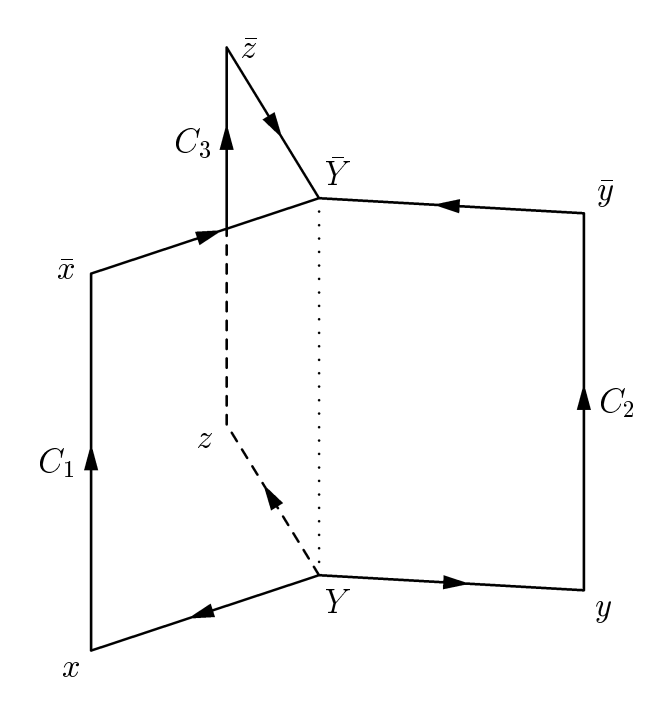


Figure 1: The baryon Wilson loop

$$\sum_{i < j} \frac{1}{2} \int_{S_i} \int_{S_j} d\sigma_{\mu_1 \nu_1}(x) d\sigma_{\mu_2 \nu_2}(x') \mathcal{D}_{\mu_1 \nu_1, \mu_2 \nu_2}(x - x') \right\}, \tag{4}$$

where \mathcal{D} designates the bilocal field strength correlators,

$$\mathcal{D}_{\mu_1\nu_1,\mu_2\nu_2}(x-x') \equiv \frac{g^2}{N_c} \operatorname{tr} \langle F_{\mu_1\nu_1}(x)\Phi(x,x')F_{\mu_2\nu_2}(x')\Phi(x',x)\rangle, \tag{5}$$

and it is assumed that the straight-line trajectories for parallel transporters are chosen. Integrations in (4) are taken over the surfaces S_i of the Wilson loop, which are formed by the trajectories of the corresponding quark, C_i , and that of the string junction, see Fig. 1. The trajectory of the string junction is shown in the figure by the dotted line.

Relying on the phenomena of the Casimir scaling [6], which is confirmed in lattice simulations, one can expect that the bilocal approximation (4) is valid within the accuracy of 1%.

Performing the surface integration in (4) and substituting the result into (1) we arrive at the expression for the baryon potential in bilocal approximation,

$$V_B(R_1, R_2, R_3) = \left(\sum_{a=b} - \sum_{a < b}\right) n_i^{(a)} n_j^{(b)} \int_0^{R_a} \int_0^{R_b} dl \, dl' \int_0^\infty dt \, \mathcal{D}_{i4, j4}(z_{ab}), \tag{6}$$

where R_a is separation of the string junction and corresponding (a-th) quark, $\mathbf{n}^{(a)}$ the unity vector directed from the string junction to this quark, and $z_{ab} = (l \, \mathbf{n}^{(a)} - l' \mathbf{n}^{(b)}, t)$.

According to MFC [7], the bilocal correlators are written in the general form containing two scalar formfactors D(z) and $D_1(z)$,

$$\mathcal{D}_{\mu_1\nu_1,\mu_2\nu_2}(z) = \left(\delta_{\mu_1\mu_2}\delta_{\nu_1\nu_2} - \delta_{\mu_1\nu_2}\delta_{\mu_2\nu_1}\right) D(z) + \frac{1}{2} \left(\frac{\partial}{\partial z_{\mu_1}} (z_{\mu_2}\delta_{\nu_1\nu_2} - z_{\nu_2}\delta_{\nu_1\mu_2}) + \frac{\partial}{\partial z_{\nu_1}} (z_{\nu_2}\delta_{\mu_1\mu_2} - z_{\mu_2}\delta_{\mu_1\nu_2})\right) D_1(z).$$
 (7)

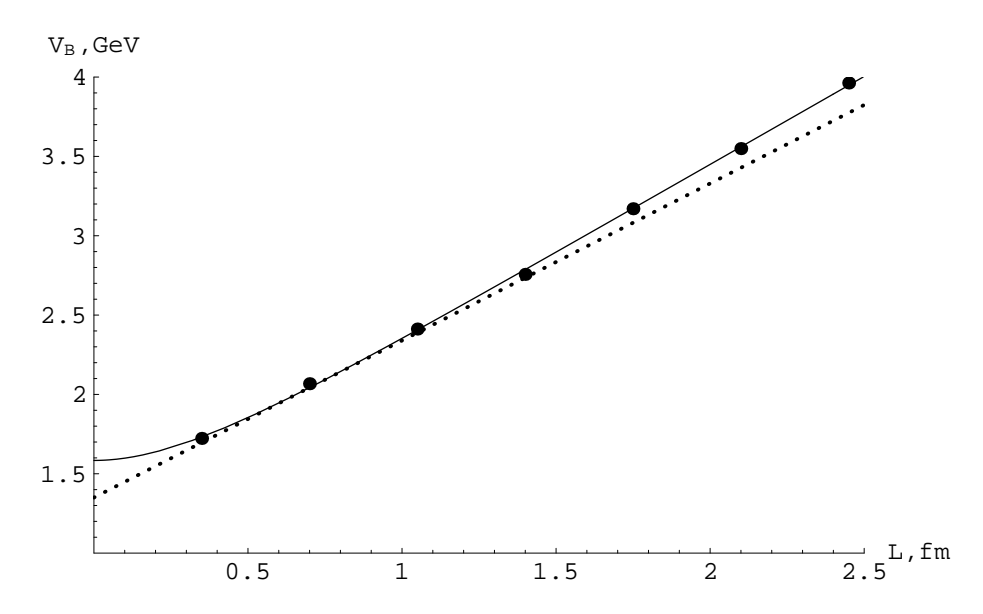


Figure 2: The lattice nonperturbative baryon potential from [2] (points) for lattice parameter $\beta = 5.8$ and MFC potential $V^{(B)}$ (solid line) with parameters $\sigma = 0.22$ GeV² and $T_g = 0.12$ fm vs. the minimal length of the string L. The dotted line is a tangent at L = 0.7 fm.

The formfactor D(z) decreases exponentially,

$$D(z) = D(0) \exp\left(-\frac{|z|}{T_g}\right),\tag{8}$$

which reflects the stochastic properties of the nonperturbative background gluon fields and is justified by the lattice computations [8]. This behavior leads to the asymptotic area law for the Wilson loop, where the string tension σ is expressed through D(z) as follows,

$$\sigma = \frac{\pi}{2} \int_0^\infty dz^2 D(z) = \pi D(0) T_g^2 = 0.18 \text{ GeV}^2.$$
 (9)

The string tension is the main nonperturbative parameter of MFC. Its value is defined phenomenologically by the slope of the meson Regge trajectories [9] and is directly related to the radius of confinement.

There is another parameter in (8), the correlation length of the background gluon field T_g . However, it is not an independent parameter. Its value is extracted from the energy of the gluon excitation of the hadron spectra [10] and may be calculated in the QCD string approach [10], [11] using the only parameter σ . The energy of the gluon excitation is large, ~ 1.5 GeV [11], and therefore the gluon correlation scale is significantly less than the confinement scale.

The formfactor $D_1(z)$ is dominated by the contribution of one-gluon-exchange of the perturbation theory, which gives rise to the static color-Coulomb potential. In the case of the baryon with the quarks forming equilateral triangle with the side r the perturbative potential reads as

$$V_{\text{pert}}(r) = -\frac{3}{2} \frac{C_F \alpha_s}{r},\tag{10}$$

where $C_F = 4/3$.

3. We now proceed to the comparison of the potential (6)-(10) with the lattice results [3], [4]. In Fig. 2 the results of the lattice simulations [3] of the baryon potential with the

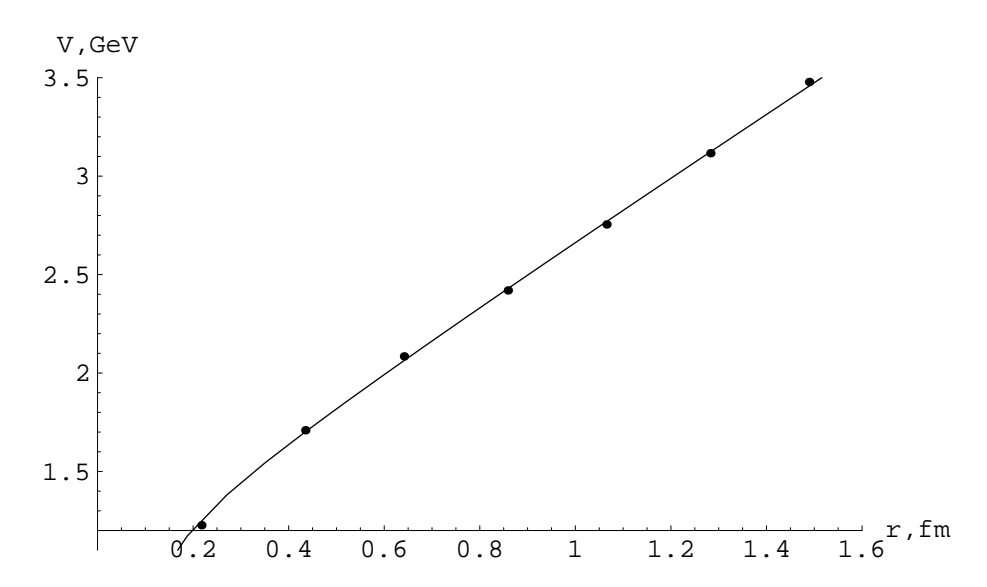


Figure 3: The lattice baryon potential in the equilateral triangle with quark separations r from [3] (points) at $\beta = 5.8$ and the MFC potential $V^{(B)} + V^{\text{pert}}_{\text{(fund)}}$ (solid line) at $\alpha_s = 0.18$, $\sigma = 0.18$ GeV², and $T_g = 0.12$ fm.

perturbative part subtracted is shown by points in dependence on the length of the string, $L = R_1 + R_2 + R_3$. Solid line in the figure shows the behavior of the nonperturbative potential calculated in MFC for the configurations of equilateral triangle. When $L \gtrsim 1$ fm, the potential grows linearly having the slope σ . When the length of the string gets smaller, the slope of the potential diminishes. Dotted line presents a tangent to the MFC potential at L = 0.7 fm. The slope of the tangent is $\sim 0.9\sigma$. Linear phenomenological potential with the same slope was used in the constituent model for the description of the spectra of baryons long time ago [1]. One can see from the figure that our curve goes well through all lattice points. The configurations of quarks forming triangles with the angles in the region the region $[\pi/20, \pi/2]$, which were used in lattice work [3], do not allow to establish any dependence of the potential on the configuration with the accuracy given. The study of the MFC potential on quark configurations will be performed below (see Fig. 4).

In Fig. 3 the results of lattice computations of the potential in equilateral triangle [4] are presented (points) vs. the quark separations r. The MFC potential with the perturbative part included is shown by solid line. One can see that all the lattice data are completely described by the MFC potential.

Computations in [3], [4] are performed in quenched approximation. In the MFC calculations sea quarks are not considered too. The studies of the effects of light dynamical quarks on the $Q\bar{Q}$ static potential in lattice were recently performed in [12]. No clear evidence for a flattening of the potential was found up to distances 2.5 fm. One can therefore expect that the sea quarks would not change the baryon potential significantly at typical hadron sizes.

It is also interesting to study the dependence of the potential in baryon on the quark locations at fixed length of the string L. Let us consider isoceles triangles with the full length of the string L and vertex γ and denote $V^L(\gamma)$ the nonperturbative potential in these triangles. At large enough sizes $L \gtrsim 1$ fm $\gg T_g$ asymptotic relations follow from (6)-(9). When $\gamma = 0$ and locations of two quarks coinside, these quarks combine in antitriplet. The string consists of one line and

$$V_1 \equiv V^L(\gamma = 0) = \sigma L - \frac{4}{\pi} \sigma T_g. \tag{11}$$

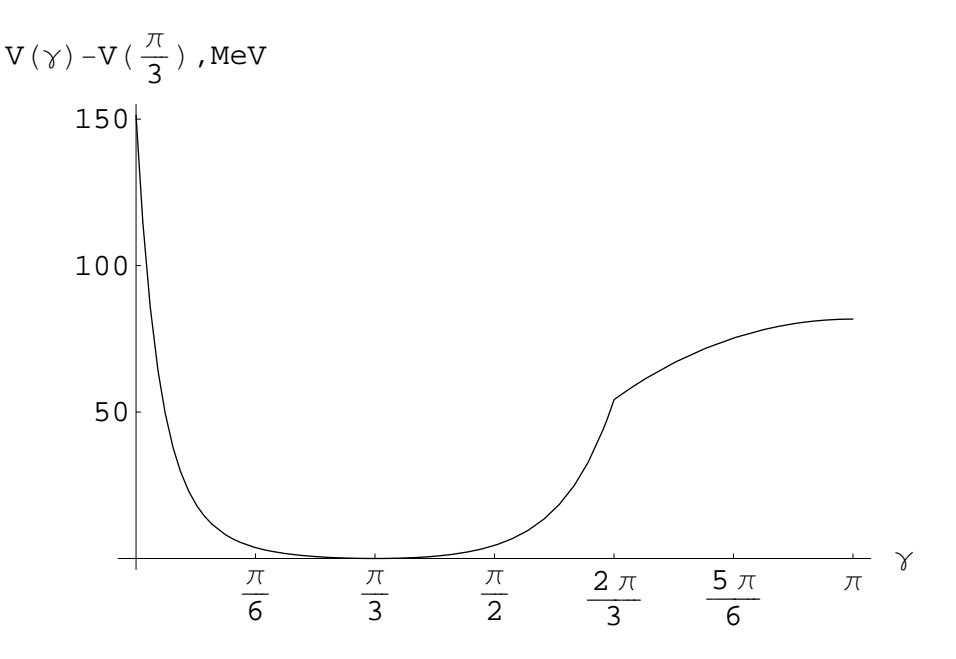


Figure 4: The baryon potential in isoceles triangle with the length of the string L=1.8 fm versus the vertex γ for $\sigma=0.18$ GeV², $T_g=0.12$ fm.

When $0 < \gamma < 2\pi/3$, the string consists of three lines, and potential

$$V_2 \equiv V^L(0 < \gamma < 2\pi/3) = \sigma L + \left(-\frac{12}{\pi} + \frac{2}{\sqrt{3}}\right) \sigma T_g.$$
 (12)

When $\gamma \geq 2\pi/3$, the string consists of two lines. In this case

$$V^{L}(\gamma \ge 2\pi/3) = \sigma L + \left(-\frac{8}{\pi} + \frac{2}{\pi}(\pi - \gamma)\operatorname{ctg}(\pi - \gamma)\right)\sigma T_{g}.$$
 (13)

It is not difficult to calculate difference between the potentials in different configurations (we use σ =0.18 GeV², T_g =0.12 fm),

$$\Delta V_1 \equiv V_1 - V_2 = \left(\frac{8}{\pi} - \frac{2}{\sqrt{3}}\right) \sigma T_g \approx 150 \text{ MeV}, \tag{14}$$

$$\Delta V_2 \equiv V^L \left(\frac{2\pi}{3}\right) - V_2 = \left(\frac{4}{\pi} - \frac{4}{3\sqrt{3}}\right) \sigma T_g \approx 55 \text{ MeV}, \tag{15}$$

$$\Delta V_3 \equiv V^L(\gamma \to \pi) - V^L\left(\frac{2\pi}{3}\right) = \left(\frac{2}{\pi} - \frac{2}{3\sqrt{3}}\right)\sigma T_g \approx 30 \text{ MeV}.$$
 (16)

In Fig. 4 the dependence of the baryon potential in isoceles triangle on the angle γ at L=1.8 fm is shown. One can verify that for the curve shown in the figure the relations (13)-(16) are justified (taking $\gamma = \pi/3$ for V_2).

The nonperturbative potential in the configurations under consideration has a pike near $\gamma=0$. However, in this region the perturbative part of the total potential dominates. Indeed, the effect reveals itself when the quark separation r_{qq} becomes less than the background correlation length. But at separation $r_{qq} \approx 0.1$ fm the color-Coulomb interaction of quarks attains 300 MeV and grows rapidly when r_{qq} diminishes. That is why to answer the question

about the relevance of quark-diquark configurations we are to consider the motion of two quarks in their perturbative potential. In particular, the radius of diquark may be estimated using the Bohr formula, $r_{qq} = 2/(m_q C_F \alpha_s)$, which yields $r_{bb} \approx 0.3$ fm and $r_{cc} \approx 1.0$ fm. More accurate values were obtained in the relativistic quark model [13], where relativistic corrections to perturbative potential as well as linear nonperturbative potential were accounted for. The radii of diquarks calculated in [13] for the ground states are $r_{bb} = 0.37$ fm, $r_{cc} = 0.56$ fm. We are to state that the radii of diquarks are comparable with the size of baryon, which perhaps signals that the formation of quark-diquark configuration is unprobable. Nevertheless, the quark-diquark approximation turns out usefull for the computations of the baryon spectra (see e.g. [13]). Account of the nonperturbative effects considered in (11)-(16) and Fig. 4 would spoil this approximation only a little.

4. To summarize, we have calculated nonperturbatively the static potential in baryon and demonstrated that it completely describes recent lattice results. The latter means in particular that the problem of the form of the potential is resolved. The potential in our approach has apparent Y-type structure, i.e. it depends only on the distances from the quarks to the string junction, the location of the latter being determined by the condition of the minimal total length of the string. The formal answer of the problem of the potential law is that the slope of the nonperturbative potential in dependence on the length of the string L grows from zero to σ when L changes from zero to ~ 1.5 fm. Therefore an effective slope at typical hadronic sizes may be chosen $\sim 0.9 \ \sigma$.

The behavior of the baryon potential considered is a consequence of two profound properties of the strong interaction, the confinement of quarks and the definite value of the correlation length of nonperturbative gluon fields. The latter is directly related to the energy scale of the gluon excitations of the hadron spectra. It is the correlation length that induces the change of the slope of the potential in baryon. Note that for mesons situation differs. The slope of the nonperturbative static potential in mesons almost does not change at small distances due to the interference with the perturbative fields [14].

Apart from the change of the slope of the potential in baryon, another related effect was studied, namely the behavior of the potential when the length of the string is fixed. It was demonstrated in particular that the difference of the potentials in configurations with the string consisting of different (one, two or three) numbers of lines turns out to be proportional to σT_g . The combination of the parameters directs immediately that the effect is induced by both the scale of confinement and correlations of gluon fields. The influence of the effect on the creation of the quark-diquark configuration is shown to be small. Last but not least, it would be interesting to study this effect in devoted lattice calculations.

The author is grateful to Yu.A.Simonov for many fruitful discussions. This work has been supported by RFBR grants 00-02-17836, 00-15-96786, and INTAS 00-00110, 00-00366.

References

- [1] S. Capstick, N. Isgur, Phys.Rev. D 34, 2809 (1986).
- [2] Yu.A. Simonov, hep-ph/0205334.
- [3] T.T. Takahashi et al., Phys.Rev. **D65**, 114509 (2002).

- [4] C. Alexandrou, Ph. de Forcrand, and O. Jahn, hep-lat/0209062, talk presented at 20th International Symposium on Lattice Field Theory (LATTICE 2002), Boston, Massachusetts, 24-29 Jun 2002.
- [5] D.S. Kuzmenko, hep-ph/0204250, Yad.Fiz. (in press).
- [6] G.S. Bali, Nucl.Phys. B (Proc.Suppl.) 83, 422 (2000);
 Yu.A. Simonov, JETP Lett. 71, 187 (2000), hep-ph/0001244;
 V.I. Shevchenko and Yu.A.Simonov, Phys.Rev.Lett. 85, 1811 (2000).
- [7] H.G. Dosch, Phys.Lett. B190, 177 (1987);
 H.G. Dosch and Yu.A. Simonov, Phys.Lett. B205, 399 (1988);
 Yu.A. Simonov, Nucl.Phys. B307, 512 (1988);
 A. Di Giacomo, H.G. Dosch, V.I. Shevchenko and Yu.A. Simonov, Phys.Rept. 372, 319 (2002).
- [8] M. Campostrini, A. Di Giacomo and G. Mussardo, Z.Phys. C25, 173 (1984);
 A. Di Giacomo and H. Panagopoulos, Phys.Lett. B285, 133 (1992);
 A. Di Giacomo, E. Meggiolaro and H. Panagopoulos, Nucl.Phys. B483, 371 (1997);
 G.S. Bali, N. Brambilla, and A. Vairo, Phys.Lett. B421, 265 (1998).
- [9] A.Yu. Dubin, A.B. Kaidalov, and Yu.A. Simonov, Phys.Lett. B323, 41 (1994); Phys.Lett. B343, 310 (1995);
 Yu.S. Kalashnikova, A.V. Nefediev, and Yu.A. Simonov, Phys.Rev. D64, 014037 (2001).
- [10] Yu.A. Simonov, Nucl. Phys. **B592**, 350 (2000).
- [11] Yu.S. Kalashnikova, D.S. Kuzmenko, this volume, hep-ph/0302070.
- [12] MILC Collaboration (C. Bernard et al.), to appear in the proceedings of 20th International Symposium on Lattice Field Theory (LATTICE 2002), Boston, Massachusetts, hep-lat/0209051;
 A. Duncan, E. Eichten, J. Yoo, hep-lat/0209123.
- [13] D. Ebert, R.N. Faustov, V.O. Galkin and A.P. Martynenko, Phys.Rev. D66, 014008 (2002).
- [14] A.M. Badalian, D.S. Kuzmenko, this volume, hep-ph/0302072.